Mathematics

https://www.aimspress.com/journal/Math

AIMS Mathematics, 11(9): 30333–30354.
DOI:10.3934/math.20261202
Received: 17 September 2025
Revised: 26 November 2025
Accepted: 09 December 2025
Published: 17 September 2026

Research article

Quadratic-phase Hilbert transform in the realm of Quaternion domains

Musadiq Shaheen[1,*], Firdous A. Shah[1], Aftab Hussain[2,*] and Hamed Alsulami[2]

[1] Department of Mathematics, University of Kashmir South Campus, Anantnag, J&K, India
[2] Department of Mathematics, King Abdulaziz University, Jeddah, Saudi Arabia

* **Correspondence:** Email: musadiqshaheen21@gmail.com, aniassuirathka@kau.edu.sa.

Abstract: In the realm of signal processing, the Hilbert transform and quadratic phase Fourier transform (QPFT) are well-established tools for analyzing complex-valued signals. However, their efficiency to analyze the quaternionic-valued signals is almost negligible due to the higher-dimensional nature of such signals. In this study, we explored this area by introducing a novel integral transform, namely, the quadratic-phase Hilbert transform in the realm of quaternion domains (briefly referred to as the quaternion quadratic-phase Hilbert transform (Q-QPHT)), by combining the merits of the Hilbert transform and QPFT. The study began with a comprehensive investigation of the fundamental properties of the proposed transform including the derivation of Parseval's formula and a detailed characterization of its range. Subsequently, general relationships, illustrative examples, and Hausdorff-Young inequalities associated with the proposed Q-QPHT were established. These findings shed light on the broader applications of the Q-QPHT in signal processing; particularly in handling complex quaternionic-valued signals that require simultaneous control over multiple aspects. Finally, the validation of the obtained results was established by well-constructed examples and numerical simulations.

Keywords: quadratic phase Fourier transform; Hilbert transform; Hausdorff-Young inequality; quaternion Fourier transform
Mathematics Subject Classification: 30G35, 42A38, 42B10, 44A15, 46S10, 47G10

1. Introduction

The Fourier transform is a powerful mathematical tool widely recognized for its applications in physics and signal processing [1]. In recent years, researchers have made significant advancements in extending the classical Fourier transform to the fractional Fourier transform (FrFT), linear canonical transform (LCT), and quadratic-phase Fourier transform (QPFT). The quadratic-phase Fourier transform, introduced by Saitoh et al. [2] in the field of mathematical signal processing, has gained significant attention in recent years as it incorporates reproducing the kernels in the form of a quadratic function within the exponent of the integral transform, allowing more accurate representation and analysis of signals with quadratic-phase components. As such, it has opened up new possibilities for signal processing techniques and has found applications in various fields such as quantum mechanics, harmonic analysis, optics, radar, sonar, communications, and image processing [3–6]. The QPFT can also be used to analyze signals that change their frequency content over time, which cannot be fully analyzed by the traditional Fourier transform. In addition, Castro et al. [7] further extended the QPFT to a more general quadratic function in the exponent, which provides a greater control over the transform and its outcomes. This broadens the applicability of the QPFT and enables researchers to tackle complex problems more effectively.

For any finite energy signal $f \in L^2(\mathbb{R})$, the quadratic-phase Fourier transform is defined by

$$\mathbb{Q}_\Lambda[f](w) = \int_{\mathbb{R}} f(t)\exp\{-i(at^2 + btw + cw^2 + dt + ew)\}dt, \tag{1.1}$$

where $\Lambda = (a, b, c, d, e)$ with real parameters.

On the other hand, the Hilbert transform (HT) is a linear operator which connects the real and imaginary parts of an analytical signal f via

$$\mathcal{H}[f](t) = \frac{1}{\pi}\int_{\mathbb{R}} \frac{f(x)}{t-x}dx, \tag{1.2}$$

that contains only non-negative frequencies of real signals and for this property, the Hilbert transform is being widely used in frequency amplitude modulation and demodulation, edge detection, signal extraction, and de-noising [8–10]. Recently Sarivastava et al. [11] intertwined the quadratic-phase Fourier transform and the classical Hilbert transform into a new integral transform, called the quadratic-phase Hilbert transform, in order to make it more robust and able to handle a wider range of signals. More precisely, the quadratic-phase Hilbert transform of any signal $f \in L^2(\mathbb{R})$ is defined by

$$H_\Lambda[f](t) = \frac{1}{\pi}\int_{\mathbb{R}} e^{i(at^2+dt-ax^2-dx)}\left\{\frac{f(x)}{b(t-x)}\right\}dx \tag{1.3}$$

with $\Lambda = (a, b, c, d, e)$ and $b > 0$. It is pertinent to mention that (1.3) reduces to the classical Hilbert transform when $\Lambda = (0, 1, 0, 0, 0)$ whereas it boils down to the fractional Hilbert transform when $\Lambda = (-\cot\alpha/2, \csc\alpha/2, -\cot\alpha/2, 0, 0)$, $\alpha \neq \pi$. Further, for $\Lambda = (-a/2b, 1/b, -c/2b, 0, 0)$, (1.3) reduces to the linear canonical Hilbert transform. This novel integral transform has the ability to extract more information and provide a more comprehensive representation of any signal in the complex plane. The quadratic-phase Hilbert transform overcomes the limitations of the classical Hilbert transform by providing a more general formulation that allows for the analysis of a wider class of signals. This new transform can also be used to analyze signals with a non-constant frequency, which is not possible with the classical Hilbert transform. The generalization of integral transforms to the quaternion setting is of importance for the study of higher dimensions, such as with the quaternion Fourier transform (QFT) [12, 13], the fractional quaternion Fourier transform (Fr-QFT) [14, 15], and the quaternion linear canonical transform (Q-LCT) [16, 17]. In the recent past, quaternion algebra has gained a respectable status in the signal processing community with its applications in color image processing, image filtering, watermarking, edge detection, and pattern recognition [18]. Significant advancements in quaternion signal processing have been reported on video and image analysis, offering efficient handling of multidimensional data like color and temporal dynamics. For instance, Zhang et al. [19] proposed a transformer-based model for video saliency prediction that enhances a single feature baseline via saliency context enhancement and incorporates temporal recurrence for long-range dependency capture, achieving superior performance on benchmark datasets. Building on such temporal mechanisms, quaternion neural networks have been adapted for image recognition tasks; Abdulqader et al. [20] demonstrated improved accuracy in color-integrated feature extraction using quaternion representations to preserve inter-channel correlations. Furthermore, Singh et al. [21] reviewed quaternion deep architectures, underscoring their efficacy in hypercomplex signal recovery and applications such as phase retrieval and tensor completion in visual domains. These developments highlight the growing relevance of quaternion-based tools in contemporary signal processing, further motivating extensions like the Q-QPHT for enhanced analytic signal generation in multidimensional contexts. Nevertheless, several recent studies have further advanced quaternion-based signal analysis by extending many prominent transforms to the quaternion domains. Ell and Sangwine established the theoretical foundation of the quaternion Fourier transform (QFT) [22], emphasizing its role in capturing multidimensional correlations among quaternionic signal components. Pei and Ding developed the fast complexified quaternion Fourier transform (CQFT) [23] to efficiently handle multidimensional color and vector-valued signals, offering computational advantages in quaternion spectral analysis. Chan et al. introduced the quaternion wavelet transform (QWT) [24] to enable multiresolution analysis in the quaternion domain, providing efficient representation for color image features and phase correlation. More recently, Chen et al. proposed the fractional quaternion cosine transform (FQCT) [25], which extends the quaternion cosine transform with a fractional parameter, offering tunable control over phase and frequency localization for color image processing tasks such as forgery detection. Motivated and inspired by these notable contributions, we aim to harness the merits of the quadratic-phase Hilbert transform for quaternion-valued signals. To the best of our knowledge, the extension of the QPHT to the quaternion domains, along with the study of its properties and important derivations for analytical signals, has not been reported yet. Interestingly, such an extension would allow the joint control of quadratic-phase modulation and analytic signal generation in the quaternion framework. Here, it is imperative to mention that our intent to formulate the quaternion quadratic-phase Hilbert transform (Q-QPHT) is firmly grounded in the facts that existing transforms such as CQFT, QWT, QFT, and FQCT primarily address frequency and spatial localization but lack the integration of a quadratic-phase kernel with the Hilbert analytic structure. Consequently, they cannot efficiently describe instantaneous frequency evolution or phase distortion in higher-dimensional quaternionic signals. The proposed quadratic phase Hilbert transform in the quaternion domain (Q-QPHT) bridges this gap by combining the analytic capabilities of the Hilbert transform with the quadratic-phase modulation of the QPFT. It preserves quaternionic non-commutativity, satisfies a Parseval-type identity ensuring energy conservation, and provides a generalized analytic framework capable of handling color, vector, and multidimensional signals with varying phase characteristics. This integration establishes the Q-QPHT as a natural extension of both the QPFT and classical Hilbert transform into the quaternion realm, offering a unified and powerful tool for advanced signal analysis. The key contributions of this article are outlined below:

- To introduce a novel quadratic-phase Hilbert transform in the realm of quaternion domains and also examine its fundamental properties as an integral transform.

- To derive several important results concerning the analysis of quaternion-valued signals via the quaternion quadratic-phase Hilbert transform.
- To validate the obtained theoretical results with well-constructed examples and numerical simulations.

The rest of the article is organized as follows: Section 2 lays the foundation with essential preliminaries that set the stage for our study. In Section 3, we introduce the novel quadratic-phase Hilbert transform in the realm of quaternion domains. Section 4 is devoted to the study of various important results pertaining to the novel integral transform. Finally, our expedition concludes with an enlightening epilogue in Section 5.

2. Preliminaries

In this section, our aim is to present an overview of the quaternion algebra and the quaternion quadratic-phase Hilbert transform, which serves as a cornerstone for the development of the subsequent sections.

2.1. Quaternion algebra

The theory of quaternions was initiated by the Irish mathematician Sir W. R. Hamilton in 1843 and is denoted by $\mathbb{H}$ in his honor. "Quaternion" means a set of 4, in which one is a real component and the other three are distinct imaginary components. The quaternion algebra $\mathbb{H}$ over $\mathbb{R}$ is given by [26]

$$\mathbb{H} := \Big\{h = h_0 + i\,h_1 + j\,h_2 + k\,h_3 \;:\; h_0, h_1, h_2, h_3 \in \mathbb{R}\Big\}, \tag{2.1}$$

where i, j, k denote both imaginary basis units of $\mathbb{H}$ and the basis for $\mathbb{R}^4$ satisfying

$$i^2 = j^2 = k^2 = ijk = -1 \text{ and } ij = k = -ji,\;\; jk = i = -kj,\; ki = j = -ik.$$

The elements i, j, k pairwise anti-commute. For a quaternion $f = h_0 + i\,h_1 + j\,h_2 + k\,h_3 \in \mathbb{H}$, h_0 is the scalar part of f denoted by $Sc[f]$ and $i\,h_1 + j\,h_2 + k\,h_3$ is called the vector (pure) part of f. Let $f_1 = h_0 + i\,h_1 + j\,h_2 + k\,h_3$ and $f_2 = p_0 + i\,p_1 + j\,p_2 + k\,p_3$ be two quaternions and then the addition $f_1 + f_2$ is defined componentwise and the multiplication is defined as

$$\begin{aligned} f_1 f_2 =&(h_0p_0 - h_1p_1 - h_2p_2 - h_3p_3) + i\,(h_0p_1 + h_1p_0 + h_2p_3 - h_3p_2)\\ &+ j(h_0p_2 - h_1p_3 + h_2p_0 + h_3p_1) + k\,(h_0p_3 + h_1p_2 - h_2p_1 + h_3p_0). \end{aligned} \tag{2.2}$$

The conjugate and norm of a quaternion $f = h_0 + i\,h_1 + j\,h_2 + k\,h_3$ are given by $\overline{f} = h_0 - i\,h_1 - j\,h_2 - k\,h_3$ and $\|f\|_{\mathbb{H}} = \sqrt{h_0{}^2 + h_1{}^2 + h_2{}^2 + h_3{}^2}$, respectively. We also note that an arbitrary quaternion h can be represented via two complex entities as $f = (h_0 + i\,h_1) + j\,(h_2 - i\,h_3) = f_1 + j\,f_2$, where $f_1, f_2 \in \mathbb{C}$, and hence, $\overline{f} = \overline{f_1} - j\,f_2$, with $\overline{f_1}$ denoting the complex conjugate of f_1. Moreover, the inner product of any two quaternions $f = f_1 + \,jf_2$ and $g = g_1 + j\,g_2$ in $\mathbb{H}$ is defined by

$$\langle f,\, g\rangle_{\mathbb{H}} = (f_1\overline{g}_1 + \overline{f}_2 g_2) + j(f_2\overline{g}_1 - \overline{f}_1 g_2). \tag{2.3}$$

By virtue of the complex domain representation, a quaternion-valued function $f : \mathbb{R}^2 \to \mathbb{H}$ can be decomposed as $f = f_1 + j\,f_2$, where f_1, f_2 are both complex-valued functions.

Let us denote by $L^2(\mathbb{R}^2,\mathbb{H})$, the space of all quaternion-valued functions f satisfying

$$\|f\|_2 = \left\{\int_{\mathbb{R}^2}\left(|f_1(\mathbf{x})|^2 + |f_2(\mathbf{x})|^2\right)d\mathbf{x}\right\}^{1/2} < \infty. \tag{2.4}$$

The norm on $L^2(\mathbb{R}^2,\mathbb{H})$ is obtained from the inner product of the quaternion-valued functions $f = f_1 + j f_2$ and $g = g_1 + j g_2$ as

$$\langle f,\, g\rangle_{\mathbb{H}} = \int_{\mathbb{R}^2}\left\{\left(f_1(\mathbf{x})\,\overline{g_1}(\mathbf{x}) + \overline{f_2}(\mathbf{x})\,g_2(\mathbf{x})\right) + j\left(f_2(\mathbf{x})\,\overline{g_1}(\mathbf{x}) - \overline{f_1}(\mathbf{x})\,g_2(\mathbf{x})\right)\right\}d\mathbf{x}.$$

An easy computation shows that $L^2(\mathbb{R}^2,\mathbb{H})$ equipped with the above-defined inner product is a Hilbert space.

Definition 2.1. *For any quaternion-valued function $f \in L^1(\mathbb{R}^2,\mathbb{H}) \cap L^2(\mathbb{R}^2,\mathbb{H})$, the right-sided quaternion Fourier transform (QFT) is denoted by $\mathcal{F}_R$ and is defined by*

$$\mathcal{F}_R[f](\mathbf{w}) = \frac{1}{2\pi}\int_{\mathbb{R}^2} f(\mathbf{t})\, e^{-it_1 w_1} e^{-jt_2 w_2}\, d\mathbf{t}, \tag{2.5}$$

where $\mathbf{t} = (t_1, t_2)$, $\mathbf{w} = (w_1, w_2)$ and the quaternion exponentials $e^{-it_1 w_1}$, and $e^{-jt_2 w_2}$ are the quaternion Fourier kernels.

The left-sided quaternion Fourier transform (QFT) is denoted by $\mathcal{F}_L$ and is defined by

$$\mathcal{F}_L[f](\mathbf{w}) = \frac{1}{2\pi}\int_{\mathbb{R}^2} e^{-it_1 w_1}\, e^{-jt_2 w_2} f(\mathbf{t})\, d\mathbf{t}, \tag{2.6}$$

whereas the two-sided quaternion Fourier transform (QFT) is defined as follows:

$$\mathcal{F}[f](\mathbf{w}) = \frac{1}{2\pi}\int_{\mathbb{R}^2} e^{-it_1 w_1} f(\mathbf{t})\, e^{-jt_2 w_2}\, d\mathbf{t}. \tag{2.7}$$

For any quaternion-valued signal $f \in L^2(\mathbb{R}^2,\mathbb{H})$, the inversion formula corresponding to (2.7) is given by

$$f(\mathbf{t}) = \frac{1}{2\pi}\int_{\mathbb{R}^2} e^{it_1 w_1}\mathcal{F}[f](\mathbf{w})\, e^{jt_2 w_2}\, d\mathbf{w}. \tag{2.8}$$

Lemma 2.1. *(QFT Parseval) The quaternion product of $f, g \in L^1(\mathbb{R}^2,\mathbb{H}) \cap L^2(\mathbb{R}^2,\mathbb{H})$ and its QFT are related by*

$$\langle f, g\rangle_{L^2(\mathbb{R}^2,\mathbb{H})} = \langle \mathcal{F}[f], \mathcal{F}[g]\rangle_{L^2(\mathbb{R}^2,\mathbb{H})}. \tag{2.9}$$

In particular, if $f = g$, we get the quaternion version of the Plancherel formula; that is,

$$\|f\|^2_{L^2(\mathbb{R}^2,\mathbb{H})} = \|\mathcal{F}[f]\|^2_{L^2(\mathbb{R}^2,\mathbb{H})}. \tag{2.10}$$

Lemma 2.2. *If $1 \le p \le 2$ and letting $\frac{1}{p} + \frac{1}{q} = 1$, for all $f \in L^p(\mathbb{R}^2,\mathbb{H})$, then it holds that*

$$\|\mathcal{F}\|_q \le (2\pi)^{\frac{1}{q}-\frac{1}{p}}\|f\|_p. \tag{2.11}$$

Next, we provide the formal definition of the two-sided quaternion quadratic-phase Fourier transform.

Definition 2.2. *The two-sided Q-QPFT of any $f \in L^1(\mathbb{R}^2, \mathbb{H}) \cap L^2(\mathbb{R}^2, \mathbb{H})$ is defined by*

$$Q_{L,R}[f](\mathbf{w}) = \int_{\mathbb{R}^2} \Lambda_L^i(t_1, w_1)\, f(\mathbf{t})\, \Lambda_R^j(t_2, w_2)\, d\mathbf{t}, \tag{2.12}$$

where $\mathbf{w} = (w_1, w_2) \in \mathbb{R}^2$ and $\mathbf{t} = (t_1, t_2) \in \mathbb{R}^2$. The parameter sets are given by

$$\mathbf{\Lambda}_L = (a_1, b_1, c_1, d_1, e_1), \qquad \mathbf{\Lambda}_R = (a_2, b_2, c_2, d_2, e_2),$$

where all parameters belong to $\mathbb{R}$ and $b_1,\ b_2 \neq 0$. $\Lambda_L^i(t_1, w_1)$ and $\Lambda_R^j(t_2, w_2)$ are the quaternion-valued kernels given by

$$\Lambda_L^i(t_1, w_1) = \sqrt{\frac{b_1 i}{2\pi}} e^{-i(a_1 t_1^2 + b_1 t_1 w_1 + c_1 w_1^2 + d_1 t_1 + e_1 w_1)},$$

and

$$\Lambda_R^j(t_2, w_2) = \sqrt{\frac{b_2 j}{2\pi}} e^{-j(a_2 t_2^2 + b_2 t_2 w_2 + c_2 w_2^2 + d_2 t_2 + e_2 w_2)}.$$

Toward the end of this section, we recall the definition of the quadratic-phase Hilbert transform.

Definition 2.3. *For a given set of real parameters $\Lambda = (a, b, c, d, e)$ with $b > 0$, the quadratic-phase Hilbert transform of any signal $f \in L^2(\mathbb{R})$ is defined by*

$$\mathcal{H}_\Lambda[f](t) = \frac{1}{\pi} \int_{\mathbb{R}} e^{i(at^2 + dt - ax^2 - dx)} \times \frac{f(x)}{b(t-x)}\, dx \tag{2.13}$$

with $\Lambda = (a, b, c, d, e)$ and $b > 0$. It is pertinent to mention that (2.13) *reduces to the classical Hilbert transform when $\Lambda = (0, 1, 0, 0, 0)$, whereas it boils down to the fractional Hilbert transform when $\Lambda = (-\cot\alpha/2, \csc\alpha/2, -\cot\alpha/2, 0, 0)$, $\alpha \neq \pi$. Further, for $\Lambda = (-a/2b, 1/b, -c/2b, 0, 0)$,* (1.3) *reduces to the linear canonical Hilbert transform.*

3. Quadratic-phase Hilbert transform in quaternion domains

In this section, our focus lies on the exploration of the two-sided Q-QPHT. Initially, we revisit the definition of the Q-QPHT and provide a lucid example to illustrate this proposed transformation. Subsequently, we demonstrate how the Q-QPHT can be simplified to the two-sided QFT. We conclude this section by outlining the essential properties of the proposed transform.

Definition 3.1. *The right-sided, left-sided, and two-sided quaternionic quadratic-phase Hilbert transforms of any $f \in L^1(\mathbb{R}^2, \mathbb{H}) \cap L^2(\mathbb{R}^2, \mathbb{H})$ are defined, respectively, as*

$$\mathcal{H}^R[f](t_1, t_2) = \int_{\mathbb{R}^2} \Lambda_L^i(x_1, t_1) \frac{f(x_1, x_2)}{(t_1 - x_1)(t_2 - x_2)} \Lambda_R^j(x_2, t_2)\, dx_1\, dx_2, \tag{3.1}$$

$$\mathcal{H}^L[f](t_1, t_2) = \int_{\mathbb{R}^2} \Lambda_L^i(x_1, t_1)\, \Lambda_R^j(x_2, t_2) \frac{f(x_1, x_2)}{(t_1 - x_1)(t_2 - x_2)}\, dx_1\, dx_2, \tag{3.2}$$

$$\mathcal{H}_{L,R}[f](t_1, t_2) = \int_{\mathbb{R}^2} \Lambda_L^i(x_1, t_1) \frac{f(x_1, x_2)}{(t_1 - x_1)(t_2 - x_2)} \Lambda_R^j(x_2, t_2)\, dx_1\, dx_2. \tag{3.3}$$

Here, the parameter sets are

$$\mathbf{\Lambda}_L = (a_1, b_1, c_1, d_1, e_1), \qquad \mathbf{\Lambda}_R = (a_2, b_2, c_2, d_2, e_2), b_1, b_2 \neq 0,$$

and the Q-QPHT kernels are given by

$$\Lambda_L^i(x_1, t_1) = \frac{1}{\pi b_1} e^{i\left(a_1 t_1^2 + d_1 t_1 - a_1 x_1^2 - d_1 x_1\right)}, \qquad \Lambda_R^j(x_2, t_2) = \frac{1}{\pi b_2} e^{j\left(a_2 t_2^2 + d_2 t_2 - a_2 x_2^2 - d_2 x_2\right)}.$$

We now present a few examples that explicitly illustrate the concept of the proposed transform.

Example 3.1. *Consider a 2D-Gaussian function* $f(\mathbf{x}) = (\mathbf{t} - \mathbf{x})\, e^{-(k_1 x_1^2 + k_2 x_2^2)}$ *with* $k_1, k_2 \geq 0$. *Then, an application of* (3.3) *yields*

$$\begin{aligned}
&\mathcal{H}_{L,R}[f(x_1, x_2)](t_1, t_2)\\
=&\frac{e^{i(a_1 t_1^2 + d_1 t_1)}}{\pi} \int_{\mathbb{R}^2} \frac{e^{-i(a_1 x_1^2 + d_1 x_1)}}{b_1(t_1 - x_1)} (\mathbf{t} - \mathbf{x}) e^{-(k_1 x_1^2 + k_2 x_2^2)} \times \frac{1}{\pi} e^{j(a_2 t_2^2 + d_2 t_2)} \frac{e^{-j(a_2 x_2^2 + d_2 x_2)}}{b_2(t_2 - x_2)}\, dx_1 dx_2\\
=&\frac{e^{i(a_1 t_1^2 + d_1 t_1)}}{\pi} \int_{\mathbb{R}} \frac{e^{-i(a_1 x_1^2 + d_1 x_1)}}{b_1(t_1 - x_1)} \times (t_1 - x_1)\, e^{-(k_1 x_1^2)} dx_1 \times \frac{1}{\pi} e^{j(a_2 t_2^2 + d_2 t_2)} \int_{\mathbb{R}} \frac{e^{-j(a_2 x_2^2 + d_2 x_2)}}{b_2(t_2 - x_2)} \times (t_2 - x_2)\, e^{-(k_2 x_2^2)} dx_2\\
=&\frac{e^{i(a_1 t_1^2 + d_1 t_1)}}{\pi b_1} \left\{ \int_{\mathbb{R}} e^{-i(a_1 x_1^2 + d_1 x_1)}\, e^{-(k_1 x_1^2)} dx_1 \right\} \left\{ \frac{e^{j(a_2 t_2^2 + d_2 t_2)}}{\pi b_2} \int_{\mathbb{R}} e^{-j(a_2 x_2^2 + d_2 x_2)} e^{-(k_2 x_2^2)} dx_2 \right\}\\
=&\frac{e^{i(a_1 t_1^2 + d_1 t_1)}}{\pi b_1} \left\{ \int_{\mathbb{R}} e^{-i a_1 x_1^2 - i d_1 x_1 - k_1 x_1^2}\, dx_1 \right\} \times \frac{e^{j(a_2 t_2^2 + d_2 t_2)}}{\pi b_2} \left\{ \int_{\mathbb{R}} e^{-j a_2 x_2^2 - d_2 x_2 j - k_2 x_2^2}\, dx_2 \right\}\\
=&\frac{e^{i(a_1 t_1^2 + d_1 t_1)}}{\pi b_1} \left\{ \int_{\mathbb{R}} e^{-(i a_1 x_1^2 + i d_1 x_1 + k_1 x_1^2)}\, dx_1 \right\} \left\{ \frac{e^{j(a_2 t_2^2 + d_2 t_2)}}{\pi b_2} \int_{\mathbb{R}} e^{-(j a_2 x_2^2 + d_2 x_2 j + k_2 x_2^2)}\, dx_2 \right\}\\
=&\frac{e^{i(a_1 t_1^2 + d_1 t_1)}}{\pi b_1} \left\{ \int_{\mathbb{R}} e^{-(k_1 + i a_1) x_1^2 + (i d_1) x_1}\, dx_1 \right\} \left\{ \frac{e^{j(a_2 t_2^2 + d_2 t_2)}}{\pi b_2} \int_{\mathbb{R}} e^{-(k_2 + a_2 j) x_2^2 + (d_2 j) x_2}\, dx_2 \right\}.
\end{aligned}$$

Using the standard Gaussian integral, we obtain

$$\mathcal{H}_{L,R} f[x_1, x_2](t_1, t_2) = \left(\frac{1}{\pi b_1} e^{i(a_1 t_1^2 + d_1 t_1)} \sqrt{\frac{\pi}{k_1 + i a_1}}\, e^{\frac{-d_1^2}{4(k_1 + i a_1)}} \right) \left(\frac{1}{\pi b_2}\, e^{j(a_2 t_2^2 + d_2 t_2)} \sqrt{\frac{\pi}{k_2 + j a_2}}\, e^{\frac{-d_2^2}{4(k_2 + j a_2)}} \right).$$

The quaternion expression has been simplified and plotted over the range -1 to 1 for t_1 and t_2. The plots represent different components shown in Figure 1 and the magnitude shown in Figure 2 of the quaternion over $[-1, 1]$.

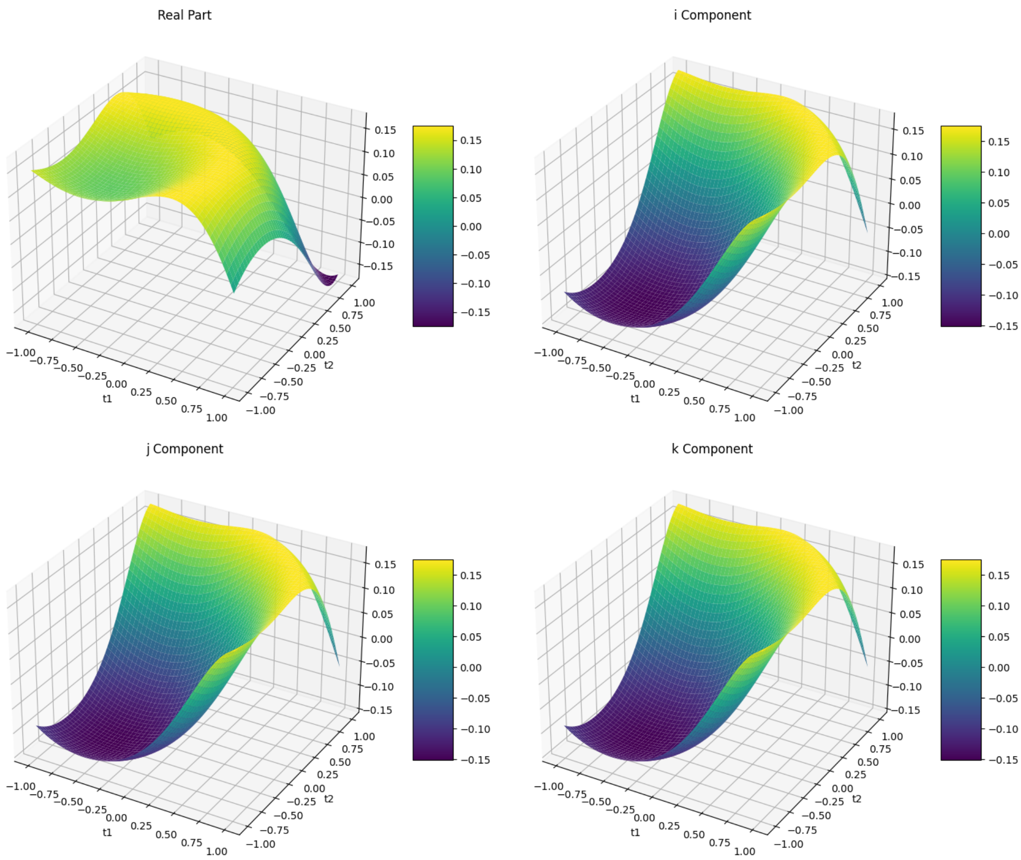

Figure 1. Different components of the quaternion over $[-1, 1]$.

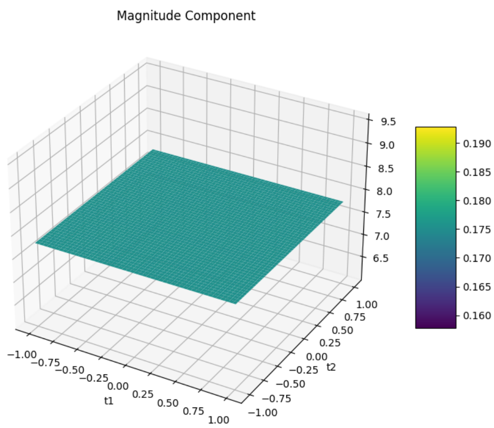

Figure 2. Magnitude of the quaternion over $[-1, 1]$.

Example 3.2. *Consider an exponential function* $f(\mathbf{x}) = e^{-\mathbf{s}(x_1+x_2)}$ *with* $\mathbf{s} = (s_1, s_2)$, $s_1, s_2 \geq 0$. *Then by definition of Q-QHPFT* (3.3), *we have*

$$\mathcal{H}_{L,R}f[x_1, x_2](t_1, t_2)$$
$$= \frac{e^{i(a_1t_1^2+d_1t_1)}}{\pi}\int_{\mathbb{R}^2}\frac{e^{-i(a_1x_1^2+d_1x_1)}}{b_1(t_1-x_1)}\,e^{-(s_1x_1+s_2x_2)}\left(\frac{e^{j(a_2t_2^2+d_2t_2)}}{\pi}\,\frac{e^{-j(a_2x_2^2+d_2x_2)}}{b_2(t_2-x_2)}\right)dx_1dx_2$$

$$=\frac{e^{i(a_1t_1^2+d_1t_1)}}{\pi}\int_{\mathbb{R}^2}\frac{e^{-i(a_1x_1^2+d_1x_1)}}{b_1(t_1-x_1)}\,e^{-is_1x_1}\left(\frac{e^{j(a_2t_2^2+d_2t_2)}}{\pi}\,\frac{e^{-j(a_2x_2^2+d_2x_2)}}{b_2(t_2-x_2)}\,e^{-js_2x_2}\right)dx_1dx_2.$$

For parameters $s_1 = d_1$ and $s_2 = d_2$, we obtain

$$\mathcal{H}_{L,R}f[x_1,x_2](t_1,t_2)=\frac{1}{\pi b_1}e^{i(a_1t_1^2+d_1t_1)}\int_{\mathbb{R}}\frac{e^{-i(a_1x_1^2+2d_1x_1)}}{b_1(t_1-x_1)}dx_1\times\frac{1}{\pi b_2}e^{j(a_2t_2^2+d_2t_2)}\int_{\mathbb{R}}\frac{e^{-j(a_2x_2^2+2d_2x_2)}}{b_2(t_2-x_2)}dx_2=I_1\times I_2, \quad (3.4)$$

where $I_1 = \dfrac{1}{\pi b_1}\,e^{i(a_1t_1^2+d_1t_1)}\displaystyle\int_{\mathbb{R}}\frac{e^{-i(a_1x_1^2+2d_1x_1)}}{b_1(t_1-x_1)}dx_1$ *and* $I_2 = \dfrac{1}{\pi b_2}\,e^{j(a_2t_2^2+d_2t_2)}\displaystyle\int_{\mathbb{R}}\frac{e^{-j(a_2x_2^2+2d_2x_2)}}{b_2(t_2-x_2)}dx_2.$

An application of Jordan's lemma and the Cauchy residue theorem yields

$$I_1 = \lim_{x_1\to t_1}(x_1-t_1)\left(\frac{e^{-i(a_1x_1^2+2d_1x_1)}}{(t_1-x_1)}\right)2i\pi = -2i\pi\,e^{-i(a_1t_1^2+2dt_1)}, \quad (3.5)$$

and

$$I_2 = \int_{\mathbb{R}}\frac{e^{-j(a_2x_2^2+2d_2x_2)}}{(t_2-x_2)}dx_2 = -2j\pi\,e^{-j(a_2t_2^2+2dt_2)}. \quad (3.6)$$

Substituting (3.5) *and* (3.6) *in* (3.4)*, we obtain*

$$\mathcal{H}_{L,R}f[x_1,x_2](t_1,t_2)=\frac{e^{i(a_1t_1^2+d_1t_1)}}{\pi b_1}\left(-2i\pi e^{-i(a_1t_1^2+2dt_1)}\right)\times\frac{e^{j(a_2t_2^2+d_2t_2)}}{\pi b_2}\left(-2j\pi e^{-j(a_2t_2^2+2dt_2)}\right)=\frac{4e^{-d(it_1+jt_2)}\mathbf{k}}{b_1b_2}.$$

The quaternion expression $e^{-(it_1+jt_2)}\mathbf{k}$ has been simplified and plotted over the range 0 to 1 for t_1 and t_2. The plots represent different components shown in Figure 3 and the magnitude shown in Figure 4 of the quaternion over [0, 1].

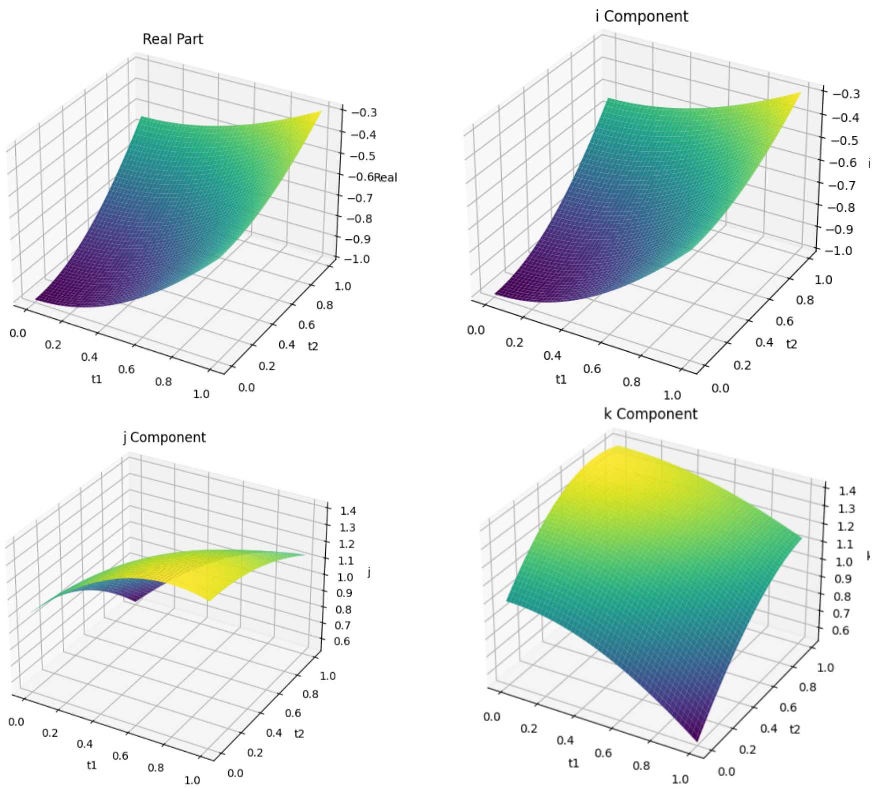

Figure 3. Different components of the quaternion over [0, 1].

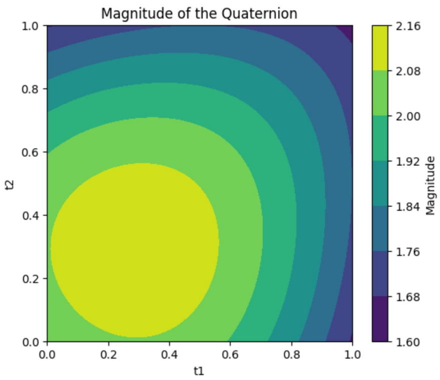

Figure 4. Magnitude of the quaternion over [0, 1].

- Real Part: This plot shows the real component of the quaternion over the t_1-t_2 space.
- i Component: This plot illustrates the component along the quaternion unit i.
- j Component: This plot visualizes the component along the quaternion unit j.
- k Component: This plot demonstrates the component along the quaternion unit k.
- Magnitude: Finally, the magnitude of the quaternion is depicted, showing how it varies across the specified range of t_1 and t_2.

Each of these components contributes to the overall quaternion value in the defined range.

The following theorem demonstrates that the quaternion-valued quadratic phase Hilbert transform shares an elegant bond with the traditional quaternion Fourier transform.

Theorem 3.1. *The quaternion quadratic-phase Hilbert transform of any quaternion-valued signal $f \in L^2(\mathbb{R}^2, \mathbb{H})$ can be reduced to the quaternion Fourier transform.*

$$\mathcal{H}_{L,R}[f](t_1,t_2) = \mathcal{F}\left[G_f(x_1,x_2)\right], \tag{3.7}$$

where

$$[G_f(x_1,x_2)] = \left[2\, e^{i(a_1t_1^2+d_1t_1)}\, e^{-ia_1x_1^2} \frac{f(x_1,x_2)}{b_1b_2(t_1-x_1)(t_2-x_2)}\, e^{-ja_2x_2^2}\ e^{j(a_2t_2^2+d_2t_2)}\right].$$

Proof. We have

$$\begin{aligned}
&\mathcal{H}_{L,R}[f](t_1,t_2)\\
=&\frac{e^{i(a_1t_1^2+d_1t_1)}}{\pi}\int_{\mathbb{R}^2} e^{-i(a_1x_1^2+d_1x_1)}\left\{\frac{f(x_1,x_2)}{b_1b_2(t_1-x_1)(t_2-x_2)}\right\} e^{-j(a_2x_2^2+d_2x_2)}\,dx_1dx_2\ e^{j(a_2t_2^2+d_2t_2)}\\
=&\frac{e^{i(a_1t_1^2+d_1t_1)}}{\pi}\int_{\mathbb{R}^2} e^{-id_1x_1}\left\{e^{-ia_1x_1^2}\frac{f(x_1,x_2)}{b_1b_2(t_1-x_1)(t_2-x_2)}\,e^{-ja_2x_2^2}\right\} e^{-jd_2x_2}\,dx_1dx_2\,e^{(ja_2t_2^2+d_2t_2)}\\
=&\frac{2\pi}{\pi}\,e^{i(a_1t_1^2+d_1t_1)}\,\mathcal{F}\left\{e^{-ia_1x_1^2}\frac{f(x_1,x_2)}{b_1b_2(t_1-x_1)(t_2-x_2)}\,e^{-ja_2x_2^2}\right\} e^{j(a_2t_2^2+d_2t_2)}\\
=&\mathcal{F}\left[2\,e^{i(a_1t_1^2+d_1t_1)}\,e^{-ia_1x_1^2}\frac{f(x_1,x_2)}{b_1b_2(t_1-x_1)(t_2-x_2)}\,e^{-ja_2x_2^2}\ e^{j(a_2t_2^2+d_2t_2)}\right]\\
=&\mathcal{F}\left[G_f(x_1,x_2)\right],
\end{aligned}$$

where

$$[G_f(x_1,x_2)] = \left[2\, e^{i(a_1t_1^2+d_1t_1)}\, e^{-ia_1x_1^2}\frac{f(x_1,x_2)}{b_1b_2(t_1-x_1)(t_2-x_2)}\, e^{-ja_2x_2^2}\ e^{j(a_2t_2^2+d_2t_2)}\right]. \tag{3.8}$$

□

In the following theorem, we obtain Parseval's identity associated with the quaternionic quadratic-phase Hilbert transform.

Theorem 3.2 (Parseval's identity)**.** *Let $f, g \in L^2(\mathbb{R}^2, \mathbb{H})$ be any two quaternion-valued signals. Then, Parseval's formula for the quadratic-phase Hilbert transform in the quaternion domain is given by*

$$\langle \mathcal{H}_{L,R}[f], g\rangle_{L^2(\mathbb{R}^2,\mathbb{H})} = \langle f, \mathcal{H}_{L,R}[g]\rangle_{L^2(\mathbb{R}^2,\mathbb{H})}\,. \tag{3.9}$$

Proof. By virtue of the definition of quaternion quadratic-phase Hilbert transform (3.3), we have

$$\begin{aligned}
&\langle \mathcal{H}_{L,R}[f], g\rangle_{L^2(\mathbb{R}^2,\mathbb{H})}\\
&= \int_{\mathbb{R}^2} \mathcal{H}_{L,R}[f](t_1,t_2)\overline{g(t_1,t_2)}dt_1dt_2\\
&= \int_{\mathbb{R}^2}\left(\frac{1}{\pi^2 b_1b_2}\int_{\mathbb{R}^2} e^{i(a_1t_1^2+d_1t_1-a_1x_1^2-d_1x_1)}\left\{\frac{f(x_1,x_2)}{(t_1-x_1)(t_2-x_2)}\right\} e^{j(a_2t_2^2+d_2t_2-a_2x_2^2-d_2x_2)}\,dx_1dx_2\right)\times\overline{g(t_1,t_2)}\,dt_1dt_2\\
&= \int_{\mathbb{R}^2}\left\{\frac{1}{\pi^2 b_1b_2}\int_{\mathbb{R}^2} e^{\overline{-i(a_1t_1^2+d_1t_1-a_1x_1^2-d_1x_1)}}\left(\overline{\overline{f(x_1,x_2)}}\right)e^{\overline{-j(a_2t_2^2+d_2t_2-a_2x_2^2-d_2x_2)}}\right\}dx_1dx_2\times\frac{\overline{g(t_1,t_2)}}{(t_1-x_1)(t_2-x_2)}dt_1dt_2.
\end{aligned}$$

We now formulate Parseval's identity for the two-sided quaternion quadratic-phase Hilbert transform by applying the cyclic multiplication symmetry, which resists the formula to scalar part only.

$$\begin{aligned}
&\langle \mathcal{H}_{L,R}[f], g\rangle_{L^2(\mathbb{R}^2,\mathbb{H})}\\
&=\frac{1}{\pi^2b_1b_2}\int_{\mathbb{R}^4}\left[f(x_1,x_2)\,\overline{\frac{g(t_1,t_2)}{(t_1-x_1)(t_2-x_2)}\, e^{-j(a_2t_2^2+d_2t_2-a_2x_2^2-d_2x_2)}}\times e^{\overline{-i(a_1t_1^2+d_1t_1-a_1x_1^2-d_1x_1)}}\right]_0 dx_1dx_2dt_1dt_2\\
&=\frac{1}{\pi^2b_1b_2}\int_{\mathbb{R}^4}\left[f(x_1,x_2)\,\overline{e^{-i(a_1t_1^2+d_1t_1-a_1x_1^2-d_1x_1)}\frac{g(t_1,t_2)}{(t_1-x_1)(t_2-x_2)}e^{-j(a_2t_2^2+d_2t_2-a_2x_2^2-d_2x_2)}}\right]_0 dx_1dx_2dt_1dt_2\\
&=\frac{1}{\pi^2b_1b_2}\int_{\mathbb{R}^2}\left[f(x_1,x_2)\,\overline{\int_{\mathbb{R}^2} e^{i(a_1x_1^2+d_1x_1-a_1t_1^2-d_1t_1)}\frac{g(t_1,t_2)}{(t_1-x_1)(t_2-x_2)}\, e^{j(a_2x_2^2+d_2x_2-a_2t_2^2-d_2t_2)}dt_1dt_2}\right]_0 dx_1dx_2\\
&=\frac{1}{\pi^2b_1b_2}\int_{\mathbb{R}^2}\left[f(x_1,x_2)\,\overline{\int_{\mathbb{R}^2} e^{i(a_1x_1^2+d_1x_1-a_1t_1^2-d_1t_1)}\frac{g(t_1,t_2)}{(x_1-t_1)(x_2-t_2)}\, e^{j(a_2x_2^2+d_2x_2-a_2t_2^2-d_2t_2)}dt_1dt_2}\right]_0 dx_1dx_2\\
&= \int_{\mathbb{R}^2}\left[f(x_1,x_2)\overline{\mathcal{H}_{L,R}[g](x_1,x_2)}\right]_0 dx_1dx_2.
\end{aligned}$$

Consequently, we obtain

$$\langle \mathcal{H}_{L,R}[f], g\rangle_{L^2(\mathbb{R}^2,\mathbb{H})} = \langle f\,, \mathcal{H}_{L,R}[g]\rangle_{L^2(\mathbb{R}^2,\mathbb{H})}\,.$$

This completes the proof of the theorem. □

In continuation, we shall derive the following important inequality pertaining to the proposed transform.

Theorem 3.3 (Hausdorff-Young inequality). *For any $f \in L^p(\mathbb{R}^2, \mathbb{H})$, $1 \leq p \leq 2$ with $\frac{1}{p} + \frac{1}{q} = 1$, the following inequality holds:*

$$\left\|\mathcal{H}_{L,R}[f](t_1, t_2)\right\|_q \leq (2\pi)^{\frac{1}{q}-\frac{1}{p}} \times \frac{2}{\mid b_1 b_2 \mid}\left\|\tilde{f}\right\|_p, \tag{3.10}$$

where $\tilde{f}(x_1, x_2) = \frac{f(x_1,x_2)}{(t_1-x_1)(t_2-x_2)}$.

Proof. From Lemma 2.2, we have

$$\|\mathcal{F}[f]\|_q \leq (2\pi)^{\frac{1}{q}-\frac{1}{p}}\|f\|_p. \tag{3.11}$$

Replacing f by $[G_f(x_1, x_2)]$,

$$\|\mathcal{F}[G_f(x_1, x_2)]\|_q \leq (2\pi)^{\frac{1}{q}-\frac{1}{p}}\|[G_f(x_1, x_2)]\|_p. \tag{3.12}$$

Now, using the definition of the quaternion quadratic-phase Hilbert transform, we have

$$\begin{aligned}
&\left\| \mathcal{H}_{L,R}[f](t_1, t_2)\right\|_q \\
\leq&(2\pi)^{\frac{1}{q}-\frac{1}{p}}\left\| 2\, e^{i(a_1 t_1^2+d_1 t_1)}\, e^{-ia_1 x_1^2} \left\{ \frac{f(x_1, x_2)}{b_1 b_2(t_1 - x_1)(t_2 - x_2)} \right\}\, e^{-ja_2 x_2^2}\, e^{j(a_2 t_2^2+d_2 t_2)} \right\|_p \\
=&(2\pi)^{\frac{1}{q}-\frac{1}{p}} \left\{ \int_{\mathbb{R}^2} \left| 2\, e^{i(a_1 t_1^2+d_1 t_1)}\, e^{-ia_1 x_1^2} \left(\frac{f(x_1, x_2)}{b_1 b_2(t_1 - x_1)(t_2 - x_2)} \right) e^{-ja_2 x_2^2}\, e^{j(a_2 t_2^2+d_2 t_2)} \right|^p dx_1 dx_2 \right\}^{\frac{1}{p}} \\
=&(2\pi)^{\frac{1}{q}-\frac{1}{p}} \left\{ \frac{2}{\mid b_1 b_2 \mid} \left(\int_{\mathbb{R}^2} \left| \frac{f(x_1, x_2)}{(t_1 - x_1)(t_2 - x_2)} \right|^p dx_1 dx_2 \right)^{\frac{1}{p}} \right\} \\
=&(2\pi)^{\frac{1}{q}-\frac{1}{p}} \left\{ \frac{2}{\mid b_1 b_2 \mid} \left(\int_{\mathbb{R}^2} \left|\tilde{f}\,(x_1, x_2)\right|^p dx_1 dx_2 \right)^{\frac{1}{p}} \right\} \\
=&(2\pi)^{\frac{1}{q}-\frac{1}{p}} \left(\frac{2}{\mid b_1 b_2 \mid}\|\tilde{f}\|_p \right),
\end{aligned}$$

where $\tilde{f}(x_1, x_2) = \frac{f(x_1,x_2)}{(t_1-x_1)(t_2-x_2)}$. □

Next, we present theorems that outline key features of the quaternion quadratic-phase Hilbert transform.

Theorem 3.4. *Let $\mathcal{H}_{L,R}[f]$ and $\mathcal{H}_{L,R}[g]$ be the quaternion quadratic-phase Hilbert transforms of any square integrable functions f and g, respectively. Then,*

(i) *Linearity:* For $\alpha, \beta \in \mathbb{C}$, we have

$$\mathcal{H}_{L,R}[\alpha\, f + \beta\, g](t_1, t_2) = \alpha\, \mathcal{H}_{L,R}[f](t_1, t_2) + \beta\, \mathcal{H}_{L,R}[g](t_1, t_2), \alpha, \beta \in \mathbb{C}.$$

(ii) *Shifting:* For $\mathbf{k} \in \mathbb{R}^2$, we have

$$\mathcal{H}_{L,R} f[\mathbf{x}-\mathbf{k}](t_1,t_2) = e^{-i(a_1k_1^2+d_1k_1)}\,\mathcal{H}_{L,R}[f]\,e^{-j(a_2k_2^2+d_2k_2)}, \mathbf{k} \in \mathbb{R}^2.$$

(iii) *Modulation:* For $w_0 = (u_0, v_0)$, we have

$$\mathcal{H}_{L,R}[M_{w_0} f](t_1,t_2) = e^{i(e_1(w_1+\frac{u_0}{e_1b_1}))}\,\mathcal{H}_{L,R}[f]\,e^{j(e_2(w_2+\frac{v_0}{e_2b_2}))}.$$

Proof. (i) To study the linearity property, we proceed as

$$\begin{aligned}
&\mathcal{H}_{L,R}[\alpha f + \beta g](t_1,t_2)\\
=&\frac{e^{i(a_1t_1^2+d_1t_1)}}{\pi}\int_{\mathbb{R}^2}\left(\frac{e^{-i(a_1x_1^2+d_1x_1)}}{b_1(t_1-x_1)}\left[\alpha(f)+\beta(g)\right]\right)\left(\frac{e^{j(a_2t_2^2+d_2t_2)}}{\pi}\,\frac{e^{-j(a_2x_2^2+d_2x_2)}}{b_2(t_2-x_2)}\right)dx_1dx_2\\
=&\frac{e^{i(a_1t_1^2+d_1t_1)}}{\pi}\int_{\mathbb{R}^2}\frac{e^{-i(a_1x_1^2+d_1x_1)}}{b_1(t_1-x_1)}\,\alpha[(f)]\frac{e^{j(a_2t_2^2+d_2t_2)}}{\pi}\,\frac{e^{-j(a_2x_2^2+d_2x_2)}}{b_2(t_2-x_2)}\,dx_1dx_2\\
&+\frac{1}{\pi}e^{i(a_1t_1^2+d_1t_1)}\int_{\mathbb{R}^2}\frac{e^{-i(a_1x_1^2+d_1x_1)}}{b_1(t_1-x_1)}\beta[(g)]\frac{e^{j(a_2t_2^2+d_2t_2)}}{\pi}\,\frac{e^{-j(a_2x_2^2+d_2x_2)}}{b_2(t_2-x_2)}\,dx_1dx_2\\
=&\alpha\,\mathcal{H}_{L,R}[f](t_1,t_2)+\beta\,\mathcal{H}_{L,R}[g](t_1,t_2).
\end{aligned}$$

(ii) Invoking the definition of the quaternion quadratic-phase Hilbert transform, we have

$$\mathcal{H}_{L,R} f[\mathbf{x}-\mathbf{k}](t_1,t_2) = \frac{e^{i(a_1t_1^2+d_1t_1)}}{\pi}\int_{\mathbb{R}^2}\left(\frac{e^{-i(a_1x_1^2+d_1x_1)}}{b_1(t_1-x_1)}\,f(\mathbf{x}-\mathbf{k})\right)\left(\frac{e^{j(a_2t_2^2+d_2t_2)}}{\pi}\frac{e^{-j(a_2x_2^2+d_2x_2)}}{b_2(t_2-x_2)}\right)dx_1dx_2.$$

Choosing $\mathbf{x}-\mathbf{k} = \mathbf{y}$, we have

$$\begin{aligned}
&\mathcal{H}_{L,R} f[\mathbf{x}-\mathbf{k}](\mathbf{t})\\
=&\frac{e^{i(a_1t_1^2+d_1t_1)}}{\pi}\int_{\mathbb{R}^2}\frac{e^{-i[a_1(y_1+k_1)^2+d_1(y_1+k_1)]}}{b_1[t_1-(y_1+k_1)]}f(y_1,y_2)\times\frac{e^{j(a_2t_2^2+d_2t_2)}}{\pi}\,\frac{e^{-j[a_2(y_2+k_2)^2+d_2(y_2+k_2)]}}{b_2[t_2-(y_2+k_2)]}dy_1dy_2\\
=&\frac{e^{i(a_1t_1^2+d_1t_1)}}{\pi}\int_{\mathbb{R}^2}\frac{e^{-i[a_1y_1^2+a_1k_1^2+2a_1y_1k_1+d_1y_1+d_1k_1]}}{b_1[t_1-(y_1+k_1)]}f(y_1,y_2)\times\frac{e^{j(a_2t_2^2+d_2t_2)}}{\pi}\,\frac{e^{-j[a_2y_2^2+a_2k_2^2+2a_2y_2k_2+d_2y_2+d_2k_2]}}{b_2[t_2-(y_2+k_2)]}\,dy_1dy_2\\
=&\frac{e^{i(a_1t_1^2+d_1t_1)}}{\pi}\int_{\mathbb{R}^2}\frac{e^{-i[a_1y_1^2+2a_1y_1k_1+d_1y_1]}}{b_1[(t_1-k_1)-y_1]}e^{-i(a_1k_1^2+d_1k_1)}f(y_1,y_2)\times\frac{e^{j(a_2t_2^2+d_2t_2)}}{\pi}\int_{\mathbb{R}^2}\frac{e^{-j[a_2y_2^2+2a_2y_2k_2+d_2k_2]}}{b_2[(t_2-k_2)-y_2]}e^{-j(a_2k_2^2+d_2k_2)}dy_1dy_2\\
=&e^{-i(a_1k_1^2+d_1k_1)}\int_{\mathbb{R}^2}\frac{1}{\pi}e^{i(a_1t_1^2+d_1t_1)}\frac{e^{-i[a_1y_1^2+2a_1y_1k_1+d_1y_1]}}{b_1[(t_1-k_1)-y_1]}f(y_1,y_2)\times\frac{e^{j(a_2t_2^2+d_2t_2)}}{\pi}\frac{e^{-j[a_2y_2^2+2a_2y_2k_2+d_2y_2]}}{b_2[(t_2-k_2)-y_2]}e^{-j(a_2k_2^2+d_2k_2)}dy_1dy_2\\
=&e^{-i(a_1k_1^2+d_1k_1)}\int_{\mathbb{R}^2}\frac{1}{\pi}e^{i(a_1t_1^2+d_1t_1)}\frac{e^{-i[a_1y_1^2+(2a_1k_1+d_1)y_1]}}{b_1[(t_1-k_1)-y_1]}f(y_1,y_2)\times\frac{e^{j(a_2t_2^2+d_2t_2)}}{\pi}\frac{e^{-j[a_2y_2^2+(2a_2k_2+d_2)y_2]}}{b_2[(t_2-k_2)-k_2]}e^{-j(a_2k_2^2+d_2k_2)}dy_1dy_2\\
=&e^{-i(a_1k_1^2+d_1k_1)}\,\mathcal{H}_{L,R}[f]\,e^{-j(a_2k_2^2+d_2k_2)},
\end{aligned}$$

where $(d_1+2a_1k_1)y_1 = {d_1}'$.
(iii) Using the definition of (3.3), we obtain

$$\mathcal{H}_{L,R}[M_{w0} f](t_1,t_2)$$

$$=\frac{e^{i(a_1t_1^2+d_1t_1)}}{\pi}\int_{\mathbb{R}^2}\left(\frac{e^{-i(a_1x_1^2+d_1x_1)}}{b_1(t_1-x_1)}\,e^{ix_1u_0}\,f(x_1,x_2)\,e^{jx_2v_0}\right)\left(\frac{1}{\pi}\,e^{j(a_2t_2^2+d_2t_2)}\,\frac{e^{-j(a_2x_2^2+d_2x_2)}}{b_2(t_2-x_2)}\right)dx_1dx_2$$
$$=\frac{1}{\pi}\int_{\mathbb{R}^2}\frac{e^{i(a_1t_1^2+d_1t_1)}}{b_1(t_1-x_1)}e^{-i(a_1x_1^2+d_1x_1+e_1w_1-e_1w_1)}e^{ix_1u_0}f(x_1,x_2)e^{jx_2v_0}\times\frac{1}{\pi}\int_{\mathbb{R}^2}\frac{e^{j(a_2t_2^2+d_2t_2)}}{b_2(t_2-x_2)}e^{-j(a_2x_2^2+d_2x_2+e_2w_2-e_2w_2)}dx_1dx_2$$
$$=\frac{1}{\pi}\int_{\mathbb{R}^2}\frac{e^{i(a_1t_1^2+d_1t_1)}}{b_1(t_1-x_1)}e^{-i(a_1x_1^2+d_1x_1+e_1(w_1-\frac{u_0}{b_1}))}e^{i(e_1(w_1+\frac{u_0}{e_1b_1}))}f(x_1,x_2)e^{i(e_2(w_2+\frac{v_0}{e_2b_2}))}\times\frac{1}{\pi}\frac{e^{j(a_2t_2^2+d_2t_2)}}{b_2(t_2-x_2)}e^{-j(a_2x_2^2+d_2x_2+e_2(w_2-\frac{v_0}{b_2}))}dx_1dx_2$$
$$=e^{i(e_1(w_1+\frac{u_0}{e_1b_1})}\frac{1}{\pi}\int_{\mathbb{R}^2}\frac{e^{i(a_1t_1^2+d_1t_1)}}{b_1(t_1-x_1)}e^{-i(a_1x_1^2+d_1x_1+e_1(w_1-\frac{u_0}{b_1}))}\times f(x_1,x_2)\frac{1}{\pi}\frac{e^{j(a_2t_2^2+d_2t_2)}}{b_2(t_2-x_2)}e^{-j(a_2x_2^2+d_2x_2+e_2(w_2-\frac{v_0}{b_2}))}e^{j(e_2(w_2+\frac{v_0}{e_2b_2}))}dx_1dx_2$$
$$=e^{i(e_1(w_1+\frac{u_0}{e_1b_1}))}\,\mathcal{H}_{L,R}[\tilde{F}]\,e^{j(e_2(w_2+\frac{v_0}{e_2b_2}))}.$$

This completes the proof of the theorem. □

4. Some important theorems associated with the QPHT in the quaternion domain

In this section, our aim is to present some fundamental results which are crucial for analyzing the analytic part of signals in the field of engineering sciences.

Theorem 4.1. *Let $\mathcal{H}_{L,R}[f]$ be the Q-QPHT of any quaternion signal $f\in L^2(\mathbb{R}^2,\mathbb{H})$ and $Q_{L,R}$ be the quaternion quadratic-phase with kernals given by $\Lambda_L^i(t_1,w_1)$ and $\Lambda_R^j(t_2,w_2)$, respectively. Then, we have*

$$Q_{L,R}[\mathcal{H}_{L,R}[f]](w_1,w_2)=i\,sgn(b_1w_1)\,Q_{L,R}[f](w_1,w_2)\,j\,sgn(b_2w_2).\tag{4.1}$$

Proof. By virtue of definition (3.3), we have

$$Q_{L,R}[\mathcal{H}_{L,R}[f]](w_1,w_2)$$
$$=\int_{\mathbb{R}^2}\Lambda_L^i(t_1,w_1)\,[\mathcal{H}_{L,R}[f]](t_1,t_2)\,\Lambda_R^j(t_2,w_2)\,dt_1dt_2$$
$$=\int_{\mathbb{R}^2}\sqrt{\frac{b_1i}{2\pi}}e^{-i(a_1t_1^2+b_1t_1w_1+c_1w_1^2+d_1t_1+e_1w_1)}\times[\mathcal{H}_{L,R}[f]](t_1,t_2)\sqrt{\frac{b_2j}{2\pi}}e^{-j(a_2t_2^2+b_2t_2w_1+c_2w_2^2+d_2t_2+e_2w_2)}\,dt_1dt_2$$
$$=\int_{\mathbb{R}^2}\sqrt{\frac{b_1i}{2\pi}}e^{-i(a_1t_1^2+b_1t_1w_1+c_1w_1^2+d_1t_1+e_1w_1)}\times\frac{1}{\pi^2b_1b_2}\int_{\mathbb{R}^2}e^{i(a_1t_1^2+d_1t_1-a_1x_1^2-d_1x_1)}$$
$$\frac{f(x_1,x_2)}{(t_1-x_1)(t_2-x_2)}e^{j(a_2t_2^2+d_2t_2-a_2x_2^2-d_1x_1)}dx_1dx_2\times\sqrt{\frac{b_2j}{2\pi}}e^{-j(a_2t_2^2+b_2t_2w_2+c_2w_2^2+d_2t_2+e_2w_2)}dt_1dt_2$$
$$=\frac{1}{2\pi^3\sqrt{b_1b_2}}\int_{\mathbb{R}^2}\int_{\mathbb{R}^2}e^{-i(b_1t_1w_1+c_1w_1^2+e_1w_1+a_1x_1^2+d_1x_1-\frac{\pi}{4})}\times\frac{f(x_1,x_2)}{(t_1-x_1)(t_2-x_2)}e^{-j(b_2t_2w_2+c_2w_2^2+e_2w_2+a_2x_2^2+d_2x_2-\frac{\pi}{4})}dx_1dx_2dt_1dt_2$$
$$=\frac{1}{2\pi\sqrt{b_1b_2}}\int_{\mathbb{R}^2}[\frac{1}{\pi}\int_{\mathbb{R}}\frac{e^{-i(b_1t_1w_1)}}{t_1-x_1}\,dt_1]\,e^{-i(c_1w_1^2+e_1w_1+a_1x_1^2+d_1x_1-\frac{\pi}{4})}$$
$$\times\,f(x_1,x_2)\,e^{-j(c_2w_2^2+e_2w_2+a_2x_2^2+d_2x_2-\frac{\pi}{4})}\,[\frac{1}{\pi}\int_{\mathbb{R}}\frac{e^{-j(b_2t_2w_2)}}{t_2-x_2}\,dt_2]\,dx_1dx_2$$
$$=\frac{1}{2\pi\sqrt{b_1b_2}}\int_{\mathbb{R}^2}[-i\,b_1sgn(b_1w_1)\,e^{-ib_1x_1w_1}]\,e^{-i(c_1w_1^2+e_1w_1+a_1x_1^2+d_1x_1-\frac{\pi}{4})}$$

$$\times\ f(x_1,x_2)e^{-j(c_2w_2^2+e_2w_2+a_2x_2^2+d_2x_2-\frac{\pi}{4})}\ \big[-j\,b_2sgn(b_2w_2)\,e^{-jb_2x_2w_2}\big]\,dx_1dx_2$$
$$=i\,sgn(b_1w_1)\int_{\mathbb{R}^2}\sqrt{\frac{b_1i}{2\pi}}e^{-i(a_1x_1^2+b_1x_1w_1+c_1w_1^2+d_1x_1+e_1w_1)}$$
$$\times\ f(x_1,x_2)\sqrt{\frac{b_2j}{2\pi}}e^{-j(a_2x_2^2+b_2x_2w_2+c_2w_2^2+d_2x_2+e_2w_2)}dx_1dx_2\quad j\,sgn(b_2w_2).$$

Equivalently,

$$Q_{L,R}[\mathcal{H}_{L,R}[f]](w_1,w_2)=i\,sgn(b_1w_1)\,Q_{L,R}[f](w_1,w_2)\,j\,sgn(b_2w_2).$$

This completes the proof of the theorem. □

Theorem 4.2. *If $\mathcal{H}_{L,R}[f]$ is the quaternionic quadratic-phase Hilbert transform and $\frac{b_1}{\sqrt{2\pi}}\overline{\Lambda_L^i(x_1,w_1)}$ and $\frac{b_2}{\sqrt{2\pi}},\overline{\Lambda_R^j(x_2,w_2)}$ are the kernels of the inverse of the Q-QPFT, then the following equality holds:*

$$\mathcal{H}_{L,R}\left[\frac{b_1b_2}{2\pi}\overline{\Lambda_L^i(x_1,w_1)}\overline{\Lambda_R^j(x_2,w_2)}\right](t_1,t_2)=\frac{1}{2\pi}\overline{\Lambda_L^i(t_1,w_1)}\Big(i\,sgn(b_1w_1)e^{ib_1t_1w_1}\Big)\Big(j\,sgn(b_2w_2)e^{jb_2t_2w_2}\Big)\overline{\Lambda_R^j(t_2,w_2)}.\tag{4.2}$$

Proof. By virtue of definition (3.3), we have

$$\mathcal{H}_{L,R}\left[\frac{b_1b_2}{2\pi}\,\overline{\Lambda_1^i(x_1,w_1)}\,\overline{\Lambda_2^j(x_2,w_2)}\right](t_1,t_2)$$
$$=\frac{1}{\pi^2b_1b_2}\int_{R^2}e^{i(a_1t_1^2+d_1t_1-a_1x_1^2-d_1x_1)}\frac{b_1b_2}{2\pi}\overline{\Lambda_1^i(x_1,w_1)}\overline{\Lambda_2^j(x_2,w_2)}\times\frac{1}{(t_1-x_1)(t_2-x_2)}e^{j(a_2t_2^2+d_2t_2-a_2x_2^2-d_2x_2)}dx_1dx_2$$
$$=\frac{1}{2\pi^3}\int_{R^2}e^{i(a_1t_1^2+d_1t_1-a_1x_1^2-d_1x_1)}\sqrt{\frac{b_1}{2\pi}}\,e^{i(a_1x_1^2+b_1x_1w_1+c_1w_1^2+d_1x_1+c_1w_1-\frac{\pi}{4})}\frac{1}{(t\_x_1)(t_2-x_2)}$$
$$\times\sqrt{\frac{b_2}{2\pi}}\,e^{j(a_2x_2^2+b_2x_2w_2+c_2w_2^2+d_2x_2+c_2w_2-\frac{\pi}{4})}\,e^{j(a_2t_2^2+d_2t_2-a_2x_2^2-d_2x_2)}\,dx_1\,dx_2$$
$$=\frac{\sqrt{b_1b_2}}{4\pi}\,e^{i(a_1t_1^2+d_1t_1+c_1w_1^2+e_1w_1-\frac{\pi}{4})}\,\frac{1}{\pi}\int_R e^{ib_1x_1w_1}\frac{dx_1}{t_1-x_1}\times\frac{1}{\pi}\int_R e^{jb_2x_2w_2}\frac{dx_2}{t_2-x_2}\,e^{j(a_2t_2^2+d_2t_2+c_2w_2^2+c_2w_2-\frac{\pi}{4})}$$
$$=\frac{1}{2\pi}e^{i(a_1t_1^2+d_1t_1+c_1w_1^2+e_1w_1-\frac{\pi}{4})}\sqrt{\frac{b_1}{2\pi}}(-i\,sgn(b_1w_1)e^{ib_1t_1w_1})\times(-j\,sgn(b_2w_2)\,e^{jb_2t_2w_2})\sqrt{\frac{b_2}{2\pi}}e^{j(a_2t_2^2+d_2t_2+c_2w_2^2+e_2w_2-\frac{\pi}{4})}$$
$$=\frac{1}{2\pi}\overline{\Lambda_1^i(t_1,w_1)}\left(i\,sgn(b_1w_1)e^{ib_1t_1w_1}\right)\left(j\,sgn(b_2w_2)e^{jb_2t_2w_2}\right)\overline{\Lambda_2^j(t_2,w_2)}.$$

This completes the proof. □

Theorem 4.3. *$\mathcal{H}_{L,R}[f]$ represents the quaternion quadratic-phase Hilbert transform $f\in L^2(\mathbb{R}^2,\mathbb{H})$. If $\frac{b_1}{\sqrt{2\pi}}\overline{\Lambda_L^i(x_1,w_1)}$, $\frac{b_1}{\sqrt{2\pi}}\overline{\Lambda_L^i(x_1,\xi_1)}$ and $\frac{b_2}{\sqrt{2\pi}}\overline{\Lambda_R^j(x_2,w_2)}$, $\frac{b_2}{\sqrt{2\pi}}\overline{\Lambda_R^j(x_2,\xi_2)}$ are kernels of the inverse of the Q-QPFT such that*

$$P_{w_1\xi_1w_2\xi_2}(x_1,x_2)=\frac{(b_1b_2)^2}{(2\pi)^2}\overline{\Lambda_L^i(x_1,w_1)}\ \overline{\Lambda_L^i(x_1,\xi_1)}\,e^{-i(a_1x_1^2+d_1x_1)}\,e^{-j(a_2x_2^2+d_2x_2)}\overline{\Lambda_R^j(x_2,\xi_2)}\ \overline{\Lambda_R^j(x_2,w_2)},$$

then, we have

$$\mathcal{H}_{L,R}[P_{w_1\xi_1w_2\xi_2}(x_1,x_2)](t_1,t_2)=\frac{4\pi^2}{b_1b_2}i\,sgn(b_1w_1+b_1\xi_1)P_{w_1\xi_1w_2\xi_2}(t_1,t_2)j\,sgn(b_2w_2+b_2\xi_2). \tag{4.3}$$

Proof. Using the definition of the Q-QPHT, we have

$$\begin{aligned}
&\mathcal{H}_{L,R}[P_{w_1\xi_1w_2\xi_2}(x_1,x_2)](t_1,t_2)\\
=&\frac{1}{\pi^2b_1b_2}\int_{\mathbb{R}^2}e^{i(a_1t_1^2+d_1t_1-a_1x_1^2-d_1x_1)}\times\frac{1}{(t_1-x_1)(t_2-x_2)}\\
&\times P_{w_1\xi_1w_2\xi_2}(x_1,x_2)e^{j(a_2t_2^2+d_2t_2-a_2x_2^2-d_2x_2)}dx_1dx_2\\
=&\frac{1}{\pi^2b_1b_2}\int_{\mathbb{R}^2}e^{i(a_1t_1^2+d_1t_1-a_1x_1^2-d_1x_1)}\times\frac{(b_1b_2)^2}{(2\pi)^2}\overline{\Lambda_1^i(x_1,w_1)}\;\overline{\Lambda_1^i(x_1,\xi_1)}\\
&\times e^{-i(a_1x_1^2+d_1x_1)}\times\frac{1}{(t_1-x_1)(t_2-x_2)}e^{-j(a_2x_2^2+d_2x_2)}\overline{\Lambda_2^j(x_2,\xi_2)}\;\overline{\Lambda_2^j(x_2,w_2)}\\
&\times e^{j(a_2t_2^2+d_2t_2-a_2x_2^2-d_2x_2)}dx_1dx_2\\
=&\frac{(b_1b_2)^2}{16\pi^4}e^{i[a_1t_1^2+d_1t_1+c_1w_1^2+e_1w_1-\pi/2+c_1\xi_1^2+e_1\xi_1]}\times\frac{1}{\pi}\int_{\mathbb{R}}e^{ib_1x_1(w_1+\xi_1)}\frac{dx_1}{(t_1-x_1)}\\
&\times\frac{1}{\pi}\int_{\mathbb{R}}e^{jb_2x_2(w_2+\xi_2)}\frac{dx_2}{(t_2-x_2)}\;e^{j[a_2t_2^2+d_2t_2+c_2w_2^2+e_2w_2-\pi/2+c_2\xi_2^2+e_2\xi_2]}\\
=&\frac{(b_1b_2)^2}{16\pi^4}e^{i[a_1t_1^2+d_1t_1+c_1w_1^2+e_1w_1-\pi/2+c_1\xi_1^2+e_1\xi_1}\\
&\times\big(-i\text{sgn}[b_1w_1+b_1\xi_1]e^{ib_1t_1(w_1+\xi_1)}\big)\big(-j\text{sgn}[b_2w_2+b_2\xi_2]e^{jb_2t_2(w_2+\xi_2)}\big)\\
&\times\;e^{j[a_2t_2^2+d_2t_2+c_2w_2^2+c_2w_2-\pi/2+c_2\xi_2^2+c_2\xi_2]}
\end{aligned} \tag{4.4}$$

Moreover we have

$$\begin{aligned}
&i\text{sgn}[b_1w_1+b_1\xi_1]\cdot P_{w_1\xi_1w_2\xi_2}(t_1,t_2)\cdot j\text{sgn}[b_2w_2+b_2\xi_2]\\
=&i\text{sgn}[b_1w_1+b_1\xi_1]\cdot\frac{(b_1b_2)^2}{(2\pi)^2}\overline{\Lambda_1^i(t_1,w_1)}\;\overline{\Lambda_1^i(t_1,\xi_1)}\,e^{-i(a_1t_1^2+d_1t_1)}\;e^{-j(a_2t_2^2+d_2t_2)}\\
&\times\overline{\Lambda_2^j(t_2,\xi_2)}\;\overline{\Lambda_2^j(t_2,w_2)}\cdot j\text{sgn}[b_2w_2+b_2\xi_2]\\
=&i\text{sgn}[b_1w_1+b_1\xi_1]\sqrt{\frac{b_1}{2\pi}}e^{i[a_1t_1^2+b_1t_1w_1+c_1w_1^2+d_1t_1+e_1w_1-\pi/4]}\\
&\times\sqrt{\frac{b_1}{2\pi}}e^{i[a_1t_1^2+b_1t_1\xi_1+c_1\xi_1^2+d_1t_1+e_1\xi_1-\pi/4]}\cdot e^{-i(a_1t_1^2+d_1t_1)}\cdot e^{-j(a_2t_2^2+d_2t_2)}\\
&\times\sqrt{\frac{b_2}{2\pi}}e^{j[a_2t_2^2+b_2t_2\xi_2+c_2\xi_2^2+d_2t_2+e_2\xi_2-\pi/4]}\sqrt{\frac{b_2}{2\pi}}e^{j[a_2t_2^2+b_2t_2w_2+c_2w_2^2+d_2t_2+e_2w_2-\pi/4]}\times j\text{sgn}[b_2w_2+b_2\xi_2]\\
=&\frac{(b_1b_2)^2}{(2\pi)^2}i\text{sgn}[b_1w_1+b_1\xi_1]\cdot e^{i[a_1t_1^2+b_1t_1(w_1+\xi_1)+c_1w_1^2+d_1t_1+e_1w_1-\pi/4]}\cdot e^{i[c_1\xi_1^2+e_1\xi_1-\pi/4]}\\
&\times e^{j[c_2\xi_2^2+e_2\xi_2-\pi/4]}\cdot e^{j[a_2t_2^2+b_2t_2(w_2+\xi_2)+c_2w_2^2+d_2t_2+e_2w_2-\pi/4]}\cdot j\text{sgn}[b_2w_2+b_2\xi_2]\\
=&\frac{4\pi^2}{b_1b_2}\cdot\frac{(b_1b_2)^2}{16\pi^4}i\text{sgn}[b_1w_1+b_1\xi_1].
\end{aligned} \tag{4.5}$$

From (4.4) and (4.5), we obtain

$$\mathcal{H}_{L,R}[P_{w_1\xi_1 w_2\xi_2}(x_1, x_2)](t_1, t_2) = \frac{4\pi^2}{b_1 b_2} i\, \mathrm{sgn}(b_1 w_1 + b_1\xi_1) P_{w_1\xi_1 w_2\xi_2}(t_1, t_2)\, j\, \mathrm{sgn}(b_2 w_2 + b_2\xi_2).$$

This completes the proof of the theorem. □

5. Numerical simulations

This section aims to elucidate the relevance of the proposed quaternion quadratic-phase Hilbert transform (Q-QPHT) within the wider domain of signal processing. Here, we shall take into consideration two aspects: first, we analyze the efficacy of the Q-QPHT in color image processing and also provide a comparative analysis with some of the existing tools of color image processing; second, our goal is to validate the 2D left-right Hilbert operator using an isotropic Gaussian input.

5.1. Comparative analysis: superiority of the quaternion quadratic-phase Hilbert transform

This subsection is devoted to analyze the efficacy of our proposed quaternion quadratic-phase Hilbert transform in color image processing. We demonstrate that the quaternion quadratic-phase Hilbert transform (Q-QPHT) has significant advantages over existing quaternionic frameworks like the quaternion fractional Hilbert transform (Q-FrHT), and the quaternion linear canonical Hilbert transform (Q-LCHT). The superiority of the Q-QPHT in the undertaken numerical simulations can be primarily attributed to the fact that the Q-QPHT is apt in modeling non-stationary signals exhibiting quadratic phase modulations, a feature vital in color image processing and multidimensional signal analysis, in general. Invoking the quaternion algebra, a color image is expressed as $f(t_1, t_2) = f_1(t_1, t_2)\mathbf{i} + f_2(t_1, t_2)\mathbf{j} + f_3(t_1, t_2)\mathbf{k}$, and its analytic form $z = f + \mathcal{H}[f]$ eliminates negative frequencies while maintaining inter-channel coherence. Note that, the classical transforms like the Q-LCHT and Q-FrHT are limited to linear or fractional phase modulations and fail to accurately represent quadratic chirps. The Q-QPHT,

$$\mathcal{H}_{L,R}[f](t_1, t_2) = \frac{1}{\pi^2 b_1 b_2} \int_{\mathbb{R}^2} e^{i(a_1 t_1^2 + d_1 t_1 - a_1 x_1^2 - d_1 x_1)} \frac{f(x_1, x_2)}{(t_1 - x_1)(t_2 - x_2)} e^{j(a_2 t_2^2 + d_2 t_2 - a_2 x_2^2 - d_2 x_2)}\, dx_1 dx_2, \tag{5.1}$$

introduces tunable quadratic and linear phase parameters (a_k, d_k, b_k) that extend both the Q-FrHT and Q-LCHT. This flexible kernel structure enhances the extraction of signal envelopes and phase accuracy, particularly for quadratic-phase or chirp-like signals. To validate these advantages, the ASTRONAUT color image (512×512) was quaternion-encoded as $q(x, y) = R(x, y)\mathbf{i} + G(x, y)\mathbf{j} + B(x, y)\mathbf{k}$ and processed using the Q-QPHT, Q-LCHT, and Q-FrHT. Edge maps were derived from the gradient of the analytic signal magnitude $|z|$. Figure 5 shows that the Q-QPHT yields sharper and more coherent color edges, especially along curved features (e.g., helmet contours), while the Q-LCHT introduces affine smearing and the Q-FrHT over-smooths transitions.

Table 1 demonstrates that in comparison to the Q-LCHT and Q-FrHT, Q-QPHT produces greater PSNR and SSIM values with lower inter-channel leakage, showing that its quadratic-phase modeling offers superior analytic signal representation and negative-frequency suppression.

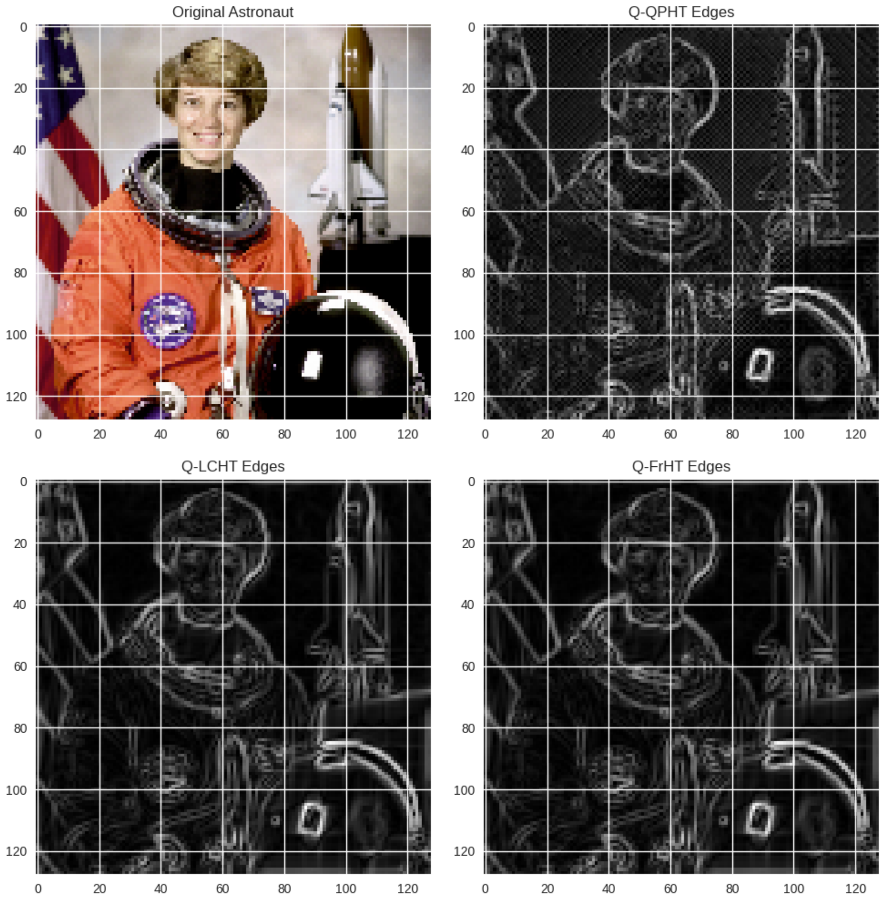

Figure 5. Edge detection comparison on the ASTROUANT image: the Q-QPHT preserves fine curved edges with minimal distortion.

Table 1. Quantitative edge detection performance on the ASTROUANT image.

Transform	PSNR (dB)	SSIM	Edge Corr. (r)	Chan. Corr. (r)
Q-QPHT	28.45	0.92	0.94	0.88
Q-LCHT	25.12	0.81	0.85	0.76
Q-FrHT	23.67	0.78	0.82	0.72

5.2. Validation of the quaternion quadratic-phase Hilbert transform

In this numerical study, we assess the efficacy of the quaternion quadratic-phase Hilbert transform (Q-QPHT) by comparing its output profile to that of the classical quaternion Hilbert transform (QHT), the quaternion fractional Hilbert transform (Q-FrHT), and the quaternion linear canonical Hilbert transform (Q-LCHT). The superiority of the Q-QPHT is demonstrated through the behavior of the transformed field and the distinct features revealed in its graphical representation as shown in Figure 6. The distinguishing features of the Q-QPHT output are briefly described below:

(1) **Enhanced Localization:** The energy of the isotropic Gaussian input is redistributed by the Q-QPHT into four distinct, symmetric, and strongly localized lobes. In contrast to this, the

- Q-LCHT generates elongated directional edges,
- Q-FrHT produces smeared oscillatory patterns,
- QHT results in diffuse and non-localized responses.

The stable quadrupole structure exhibited by the Q-QPHT demonstrates its stronger spatial localization ability relative to the other comparative transforms.

(2) **Cleaner Analytic-Signal Behavior:** The magnitude profiles demonstrate that there is no evidence of negative-frequency leakage and that the Q-QPHT generates a clear center drop. It maintains a clean, steady, and crisp positive-frequency structure. In contrast, other quaternion Hilbert-type transforms often display either mixed-phase distortions, or unwanted negative-frequency remnants. As a result, the quadratic phase of the Q-QPHT demonstrates superior analytic-signal properties.

(3) **Directional Sensitivity Through the Quadratic Phase:** The Q-QPHT accurately responds to second-order geometric variations. The anisotropy introduced by the parameters $(a_1, a_2) = (2.0, 0.5)$ appears clearly in the output, and we can observe that the structure is compressed along t_1, whereas it is elongated along t_2. Such curvature-sensitive modulation is not achievable through the Q-LCHT or the Q-FrHT. This demonstrates the superior directional flexibility provided by the quadratic phase in the proposed transform.

(4) **Energy Preservation with Structured Redistribution:** Although the input Gaussian contains a single isotropic peak, the Q-QPHT preserves its overall energy distribution while organizing it into four balanced lobes. On the other hand, the comparative transforms tend to distort global structure, or introduce oscillatory artifacts. Hence, we infer that the Q-QPHT maintains strong symmetry and controlled spreading, thereby ensuring stable and interpretable output behavior.

(5) **Improved Feature Extraction:** The quadrupole pattern generated by the Q-QPHT acts as an effective phase-sensitive edge-enhancement mechanism. It highlights curvature and directional variations more distinctly than the competing tools like the Q-LCHT, Q-FrHT, or QHT, thereby making the Q-QPHT particularly useful for two-dimensional quaternionic signal analysis.

(6) **Parameter-Controlled Flexibility:** It is imperative to highlight that the chirp parameters (a_1, a_2) provide substantial tunability. Increasing a_1 results in a stronger compression along the t_1-axis, whereas decreasing a_2 leads to an expanded structure along t_2. This parameter-driven behavior is far more expressive than the linear or fractional phase modulations offered by the existing transforms.

Based on the above-cited observations, we conclude that the Q-QPHT produces smoother, cleaner, and more interpretable graphical results than the competing quaternion Hilbert-type transforms. Its strong localization, distinct quadrupole structure, absence of negative-frequency artifacts, and parameter-based flexibility confirm the Q-QPHT as a robust and superior operator for quaternionic signal analysis. The observations remain consistent across parameter variations, indicating stability of the proposed transform.

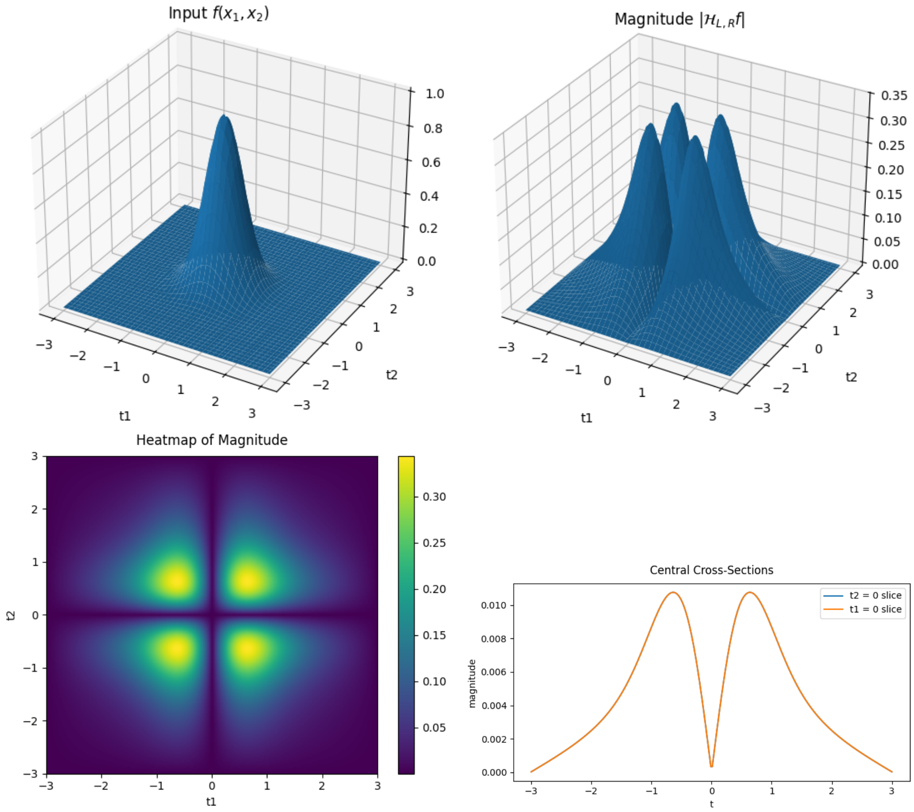

Figure 6. Graphical validation of the Q-QPHT: (Top-left) Input surface. (Top-right) Magnitude surface. (Bottom-left) Heatmap of the magnitude. (Bottom-right) Central cross-sections.

6. Conclusions

In this study, we have accomplished three major objectives: first, we introduced the quaternionic quadratic-phase Hilbert transform as a novel tool for analyzing quaternionic signals. Second, we have established the fundamental properties of the Q-QPHT, including Parseval's formula, linearity, shift, and modulation, also we derived some crucial results for analyzing the analytic part of signals in engineering sciences. Finally, to validate the obtained results, simulation results were proposed.The results show that the methods presented in the paper are correct and effective. The obtained results are of substantial importance and serve as a valuable heuristic reference for the mathematical and signal processing communities. This study enhances the understanding and application of quaternionic signal processing techniques, offering meaningful insights and improved analytical tools for complex-valued signals.

Author contributions

Musadiq Shaheen conceived the main idea and methodology, performed the analysis, conducted the numerical experiments, and wrote the manuscript; Firdous A. Shah supervised the research and critically reviewed the manuscript; Aftab Hussain and Hamed Alsulami provided valuable suggestions to improve the results, which greatly enhanced the quality of the manuscript, and contributed to editing and revising the manuscript. All authors read and approved the final version.

Use of Generative-AI tools declaration

The authors declare they have not used Artificial Intelligence (AI) tools in the creation of this article.

Acknowledgments

The authors thanks to the employer of King Abdulaziz University, Jeddah, Saudi Arabia for their financial support and encouragement.

Conflict of interest

The authors declare no conflict of interest.

References

1. R. Bracewell, *The Fourier transform and its applications*, Boston: McGraw Hill, 2000.
2. S. Saitoh, Theory of reproducing kernels: applications to approximate solutions of bounded linear operator functions on Hilbert spaces, In: *Selected papers on analysis and differential equations*, Providence: American Mathematical Society, 2010, 107–134. https://doi.org/10.1090/trans2/230/06
3. L. Castro, L. Minh, N. Tuan, New convolutions for quadratic-phase Fourier integral operators and their applications, *Mediterr. J. Math.*, **15** (2018), 13. https://doi.org/10.1007/s00009-017-1063-y
4. M. Kumar, T. Pradhan, Quadratic-phase Fourier transform of tempered distributions and pseudo-differential operators, *Integr. Transf. Spec. F.*, **33** (2022), 449–465. https://doi.org/10.1080/10652469.2021.1944132
5. F. A. Shah, W. Z. Lone, Quadratic-phase wavelet transform with applications to generalized differential equations, *Math. Method. Appl. Sci.*, **45** (2022), 1153–1175. https://doi.org/10.1002/mma.7842
6. M. Shaheen, F. Shah, Generalized 2D Hilbert quadratic-phase transform with applications to wrapped phase map determination, *Circ. Syst. Signal Proc.*, **45** (2026), 7086–7108. https://doi.org/10.1007/s00034-026-03493-7
7. L. P. Castro, M. R. Haque, M. M. Murshed, S. Saitoh, N. M. Tuan, Quadratic Fourier transforms, *Ann. Funct. Anal.*, **5** (2014), 10–23. https://doi.org/10.15352/afa/1391614564
8. A. W. Lohmann, D. Mendlovic, Z. Zalevsky, Fractional Hilbert transform, *Opt. Lett.*, **21** (1996), 281–283. https://doi.org/10.1364/OL.21.000281
9. H. Stark, An extension of the Hilbert transform product theorem, *Proc. IEEE*, **59** (1971), 1359–1360. https://doi.org/10.1109/PROC.1971.8420
10. A. I. Zayed, Hilbert transform associated with the fractional Fourier transform, *IEEE Signal Proc. Lett.*, **5** (1998), 206–208. https://doi.org/10.1109/97.704973

11. H. M. Srivastava, F. A. Shah, H. L. Qadri, W. Z. Lone, M. S. Gojree, Quadratic-phase Hilbert transform and the associated Bedrosian theorem, *Axioms*, **12** (2023), 218. https://doi.org/10.3390/axioms12020218
12. Y. X. Fu, L. Q. Li, Paley-Wiener and Boas theorems for the quaternion Fourier transform, *Adv. Appl. Clifford Algebras*, **23** (2013), 837–848. https://doi.org/10.1007/s00006-013-0412-6
13. E. Hitzer, Quaternion Fourier transform on quaternion fields and generalizations, *Adv. Appl. Clifford Algebras*, **17** (2007), 497–517. https://doi.org/10.1007/s00006-007-0037-8
14. D. Y. Wei, Y. M. Li, Different forms of Plancherel theorem for fractional quaternion Fourier transform, *Optik*, **124** (2013), 6999–7002. https://doi.org/10.1016/j.ijleo.2013.05.163
15. G. L. Xu, X. T. Wang, X. G. Xu, Fractional quaternion Fourier transform, convolution and correlation, *Signal Process.*, **88** (2008), 2511–2517. https://doi.org/10.1016/j.sigpro.2008.04.012
16. K. I. Kou, J. Morais, Asymptotic behaviour of the quaternion linear canonical transform and the Bochner-Minlos theorem, *Appl. Math. Comput.*, **247** (2014), 675–688. https://doi.org/10.1016/j.amc.2014.08.090
17. K. I. Kou, J. Y. Ou, J. Morais, On uncertainty principle for quaternionic linear canonical transform, *Abstr. Appl. Anal.*, **2013** (2013), 725952. https://doi.org/10.1155/2013/725952
18. C. Huang, J. Li, G. Gao, Review of quaternion-based color image processing methods, *Mathematics*, **11** (2023), 2056. https://doi.org/10.3390/math11092056
19. Y. Z. Zhang, Y. G. Xiao, Y. K. Zhang, T. Zhang, Video saliency prediction via single feature enhancement and temporal recurrence, *Eng. Appl. Artif. Intel.*, **160** (2025), 111840. https://doi.org/10.1016/j.engappai.2025.111840
20. T. Y. Abdulqader, S. A. Abdulqader, S. A. Baker, Enhancing image recognition with quaternion neural networks: a novel approach to color layer integration, *Journal of Image and Graphics*, **13** (2025), 190–197. https://doi.org/10.18178/joig.13.2.190-197
21. S. Singh, S. Kumar, B. K. Tripathi, A comprehensive analysis of quaternion deep neural networks: architectures, applications, challenges, and future scope, *Arch. Comput. Method. Eng.*, **32** (2025), 2607–2634. https://doi.org/10.1007/s11831-024-10216-1
22. E. Hitzer, Quaternion Fourier transform, In: *Quaternionic integral transforms*, Cham: Birkhäuser, 2023, 1–58. https://doi.org/10.1007/978-3-031-28375-8_1
23. S. Said, N. Le Bihan, S. J. Sangwine, Fast complexified quaternion Fourier transform, *IEEE Trans. Signal Proces.*, **56** (2008), 1522–1531. https://doi.org/10.1109/TSP.2007.910477
24. E. Bayro-Corrochano, The theory and use of the quaternion wavelet transform, *J. Math. Imaging Vis.*, **24** (2006), 19–35. https://doi.org/10.1007/s10851-005-3605-3
25. B. Chen, M. Yu, Q. Su, L. Li, Fractional quaternion cosine transform and its application in color image copy-move forgery detection, *Multimed. Tools Appl.*, **78** (2019), 8057–8073. https://doi.org/10.1007/s11042-018-6595-z
26. J. Morais, S. Georgiev, W. Sprobig, *Real quaternionic calculus handbook*, Basel: Birkhäuser, 2014. https://doi.org/10.1007/978-3-0348-0622-0

AIMS Press